Cosmic radiation effects on high-voltage semiconductors in automotive onboard chargers

Mission profile and FIT rate assessment

About this document

Scope and purpose

This document gives an introduction to the cosmic radiation failure mechanism. Additionally, it describes the influencing factors of the application on the failure rate, and gives concrete results of robustness validation based on a generic mission profile.

Intended audience

This document is intended for hardware design engineers for high-voltage (HV) power electronic systems in plug-in hybrid and battery electric vehicles.

Table of contents

1 Introduction

Quality and reliability specialists often describe the lifetime of a population of products using the graphical representation in **Figure 1**, commonly known as the bathtub curve. The bathtub curve consists of three periods: an infant mortality period with a decreasing failure rate; followed by a normal life period (also known as “useful life”) with a low, relatively constant failure rate; and concluding with a wear-out period that exhibits an increasing failure rate. Infant mortality failures can be brought down to a negligible value by adopting the proper test procedures, while wear-out failures are not a concern because, when the product is well designed, they will happen only after the end of the specified lifetime. On the other hand, random failures, as the name suggests, happen randomly throughout the lifetime of the product and therefore their failure rate is constant. This kind of failure is therefore the main contributor to the observed failure rate during the useful life of the product.

While all of this applies to products in general, the focus here is on power electronic components, and more specifically on HV MOSFETs. At Infineon, the highest product quality is ensured through the introduction of a number of tests at wafer and package level to screen for infant mortality failures.

Single-event burnouts (SEBs) caused by cosmic radiation contribute to the random failure rate in HV MOSFETs. Even though the event is random, its probability can be predicted by knowing the application conditions. This application note will provide a simple introduction to SEBs and a basic approach to estimate the cosmic radiation failure rate of a HV MOSFET used in a given application.

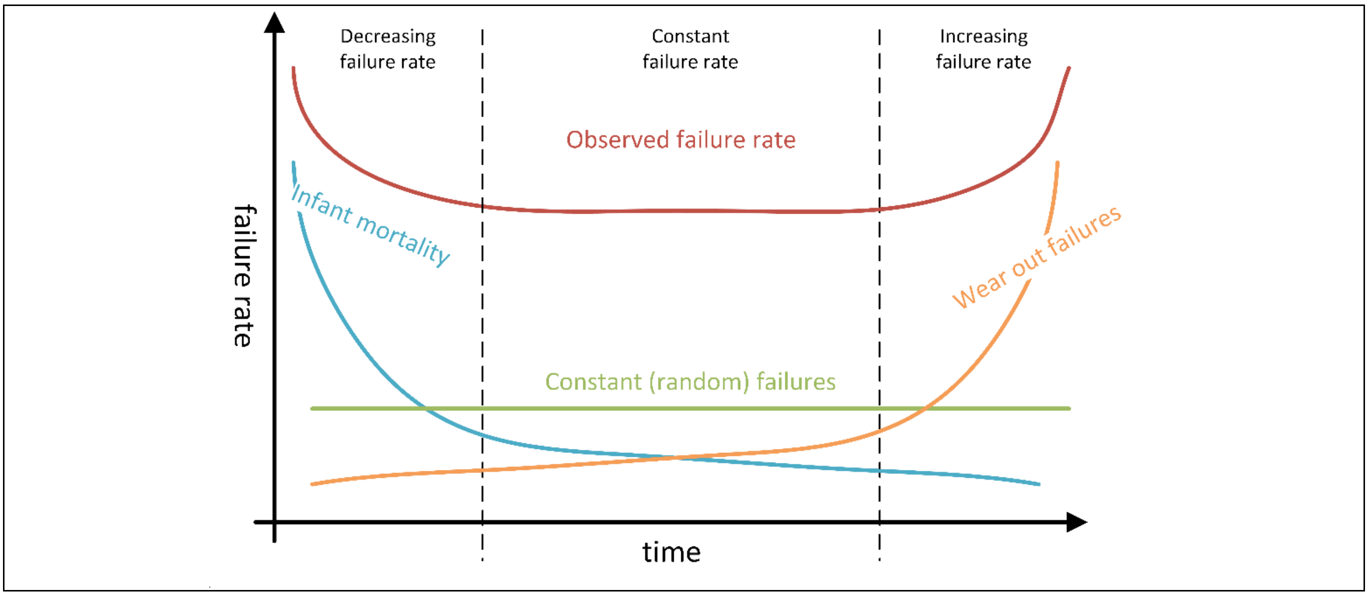

Figure 1 **The bathtub curve: typical failure rate of an entire population of products over time**

1.1 What is cosmic radiation?

Cosmic radiation bombards the Earth with highly energetic particles – mainly protons, light, and heavy nuclei. In rare events, particle energies up to the extremely high values of 10^{20} eV have been observed [1]. Upon impact with the Earth’s atmosphere, they collide with atomic nuclei in the outer atmosphere. These collisions create a multitude of secondary particles, which carry away the energy of the primary particles.

Generally, these secondary particles have sufficient energy to create even more particles in the subsequent collisions. Consequently, avalanche multiplication takes place while at the same time the particle intensity is reduced by absorption in the atmosphere. A detailed description of this process can be found in [2] and is schematically represented in **Figure 2**.

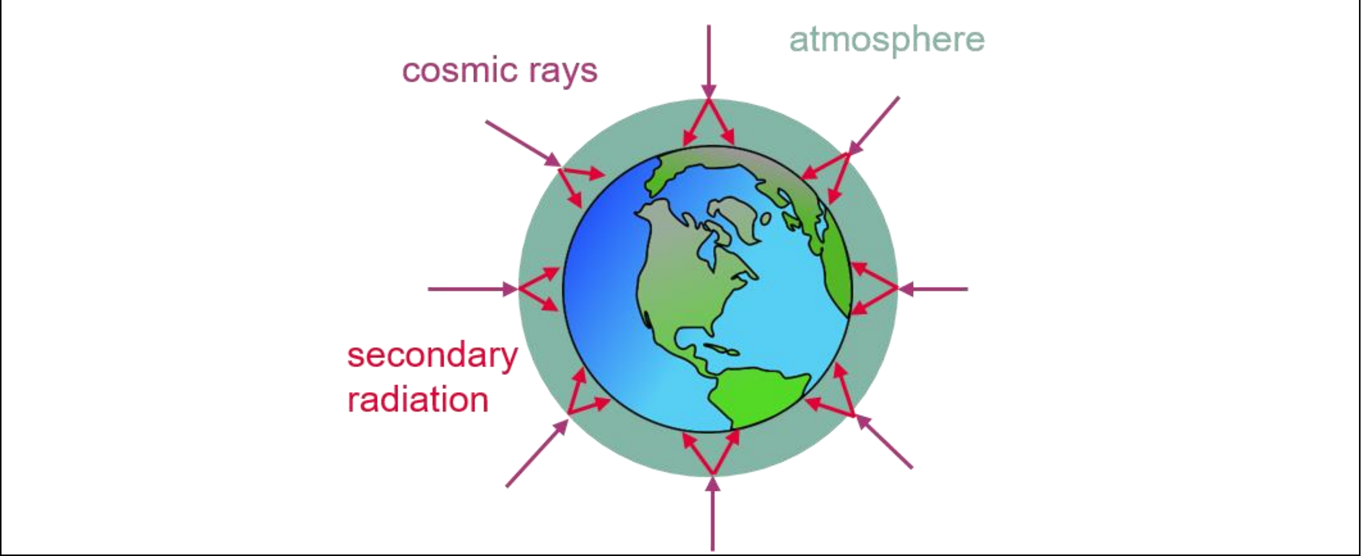

Figure 2 **Schematic representation of cosmic radiation impact on Earth's atmosphere**

1.2 How do cosmic rays affect power electronics?

As secondary cosmic particles arrive at the Earth's surface, they interact with the dense matter on the ground. For a HV MOSFET device, this means that there is a certain probability of being hit by such a particle in the blocking region, as shown in **Figure 3**. In that event, the particle eventually transfers its energy (typically from several tens to several hundred of MeV; 100 MeV ≈ 16 pJ) to the device, creating electron-hole pairs over a distance of some micrometers. The spectrum and composition of the secondary cosmic radiation particles show that neutrons are by far the most harmful component, because they are the only type of particle present in sufficient numbers and at the same time capable of transferring all their energy in one single spot [3].

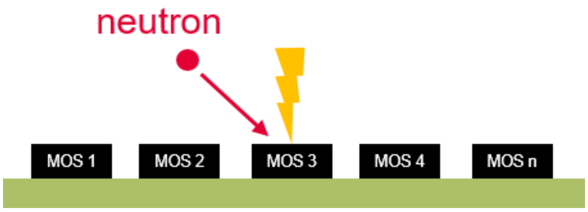

Figure 3 **Neutron impacting a MOSFET soldered onto a PCB**

Next, a simple explanation of the SEB failure mechanism is shown. For the sake of simplicity, a simple p-n junction is considered instead of the much more complex structure of a superjunction device. **Figure 4** represents the electric field profile of a reverse-biased p-n junction at the instant right before the impact of the intruding neutron.

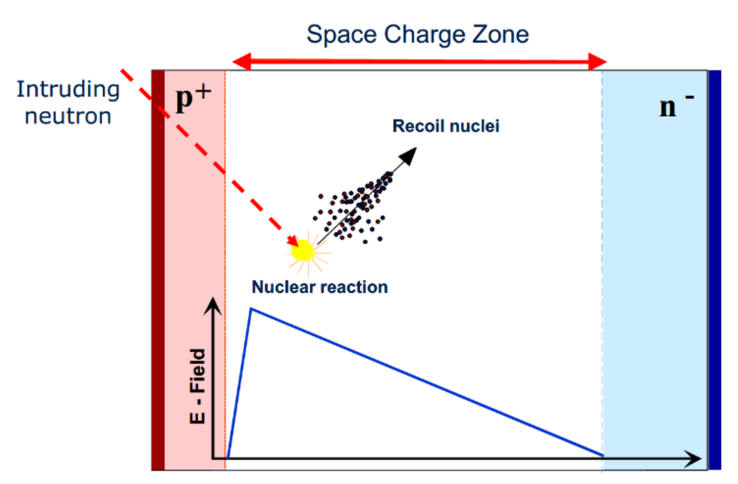

Figure 4 **Electric field profile throughout the space charge zone of a p-n junction before the neutron impact**

An intruding neutron creates a recoil ion when colliding with a silicon nucleus of the power device. The ion in turn deposits its kinetic energy and creates a highly localized burst of charge over a distance of some micrometers. In the field zone of a device in the blocking state this plasma of charge carriers shields its interior from the electric field, as shown in **Figure 5**. At the edges of the plasma zone, high field peaks build up. Due to the corresponding impact ionization, the field peaks start propagating through the entire device length and are thereby extending the plasma zone. This self-sustaining process is called a “streamer”. This highly conductive filament (streamer) is electrically shorting source and drain. The subsequent self-heating can cause the silicon to melt, resulting in the destruction of the device. [3]

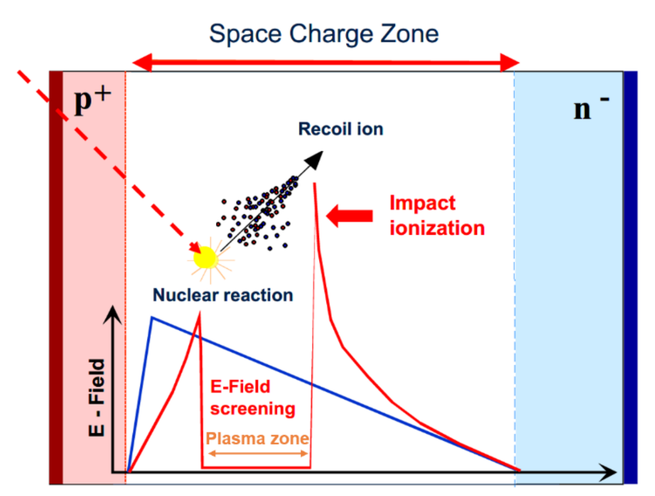

Figure 5 **Electric field profile throughout the space charge zone of a p-n junction after the intruding neutron impact**

As the destruction mechanism is driven by impact ionization, it is obvious that in the conduction state, where high electric fields are not present, some extra charge carriers will cause no harm and can therefore be ignored when assessing the failure rates.

2 FIT and ppm rate

The failures-in-time (FIT) of a device is the number of failures that can be expected in one billion device-hours of operation, and it is typically specified per unit area (e.g., 0.01 FIT/mm^2) or per device (e.g., 1 FIT/device). It can be derived from experimental measurements as follows:

$$FIT = \frac{F}{N \cdot T} \cdot 10^9$$

Where:

- N: total number of tested devices
- F: number of devices which failed
- T: total test time in hours

A simplified example of FIT curves of MOSFETs belonging to different **CoolMOS™** families is shown in **Figure 6**; here the exponential dependency of the FIT with the blocking voltage can be observed.

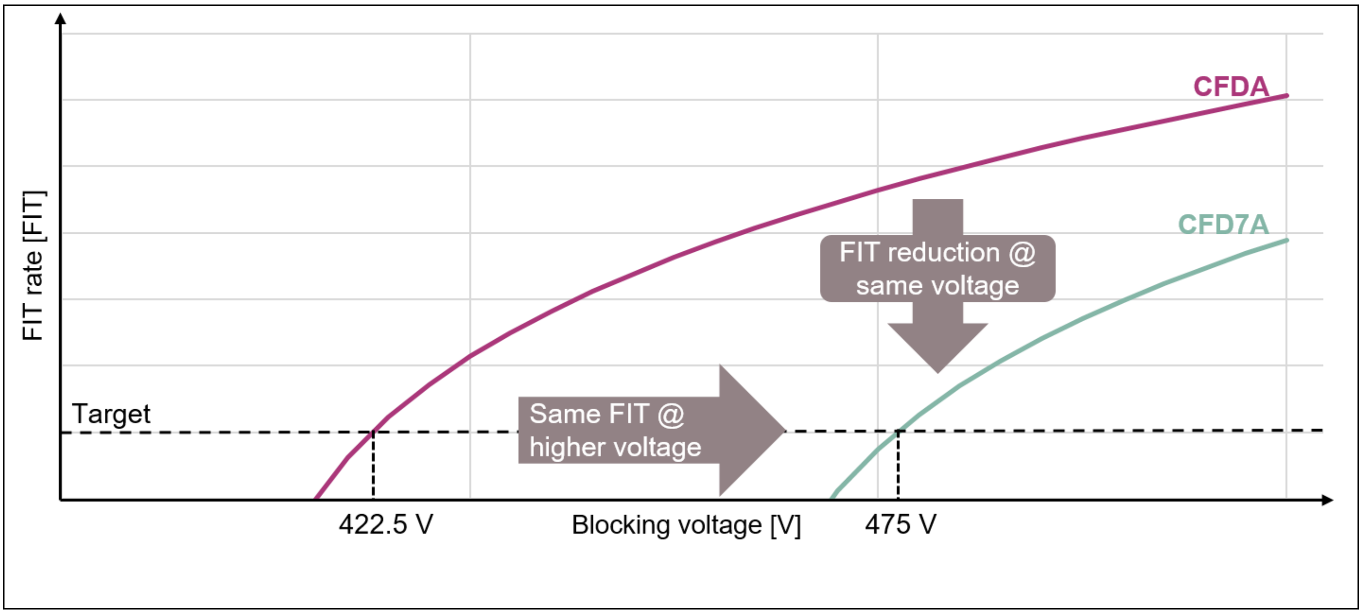

Figure 6 **Schematic representation of FIT curve of CoolMOS™ CFDA and CoolMOS™ CFD7A in semi-logarithmic scale**

The failure rate can also be expressed in parts per million (ppm). This number represents the number of failures per million parts after a defined amount of time, and it can be calculated as follows:

$$failure\ rate\ in\ ppm = \frac{F}{N} \cdot 10^6$$

It is important to emphasize that while the FIT does not depend on the total lifetime (LT) of the device, the ppm failure rate does. The relationship between these two quantities is the following:

$$failure\ rate\ in\ ppm = \frac{FIT \cdot LT}{10^3}$$

For instance, assuming a technology with a FIT of 0.01, the failure rate is 0.1 ppm if the considered lifetime is 10000 h, while it is 1 ppm if the considered lifetime is extended to 100000 h.

2.1 What does the FIT rate depend on?

The FIT rate curves are typically specified per unit area at ambient temperature (T_{amb} = 25°C) and at zero meters above sea level. This already implicitly highlights the basic FIT dependencies:

- **Blocking voltage:** The drain-source voltage blocked by the device during the off-state determines the electric field in the interior of the device. As the destruction mechanism is driven by impact ionization, the FIT has an exponential dependence on the applied drain-source blocking voltage. Therefore, the sensitivity to this parameter is extremely high. An example of this dependency is shown in **Figure 6**.
- **Altitude:** Due to the higher flux of particles at elevated altitudes, the failure rate is increasing. As shown in **Figure 7**, the FIT dependency on the altitude is exponential (rule of thumb: the FIT at 3000 m above sea level is one order of magnitude higher than the FIT at sea level).
- **Junction temperature (T_j):** The FIT dependency on the temperature is negative, meaning that higher temperature results in lower FIT (rule of thumb: the FIT at T_j = 150°C is one order of magnitude lower than at T_j = 25°C.
- **Chip area:** The FIT dependency on the chip area is linear. It is clear that the rate at which fatal hits happen is directly proportional to the area over which a neutron can penetrate.
- **Device on- and off-state:** The FIT exhibits a linear dependency on the time during which the device is in the off-state. In other words, it linearly depends on the duty cycle.

2.2 How to measure single device cosmic ray failure rate

2.2.1 Measurements under natural radiation environment

The easiest way to measure the cosmic radiation-induced failure rate of a given device technology is by carrying out storage experiments. The FIT can be estimated by reverse biasing with a known drain-source V_{DS} voltage a number of devices under test (DUTs) having the same part number, and waiting for failures to happen.

Variations of parameters such as the reverse voltage V_{DS} and the temperature require separate runs, one for each combination of parameters. This approach is only feasible for sufficiently high failure rates usually only obtained close to the drain-source breakdown voltage $V_{(BR)DSS}$.

Unfortunately, it is not possible to define a “voltage acceleration factor” to determine the device failure rate at lower application-relevant voltage levels from measurements close to $V_{(BR)DSS}$ of the device; therefore the failure rates also have to be measured at lower voltages. This is why accelerated testing, in particular, at artificial radiation sources becomes necessary, to avoid years of measurement time and/or an excessively large number of DUTs.

2.2.2 Accelerated measurements

At high elevations, the flux of cosmic radiation increases. Therefore, high-altitude testing offers an acceleration compared to sea level testing. The advantage of this approach is the presence of a realistic spectrum of cosmic neutrons, and several manufacturers use this approach by testing for example at the German mountain Zugspitze (2962 m above sea level). The drawback of such an approach is relative inaccessibility and an acceleration factor hardly above 10 (see **Figure 7**).

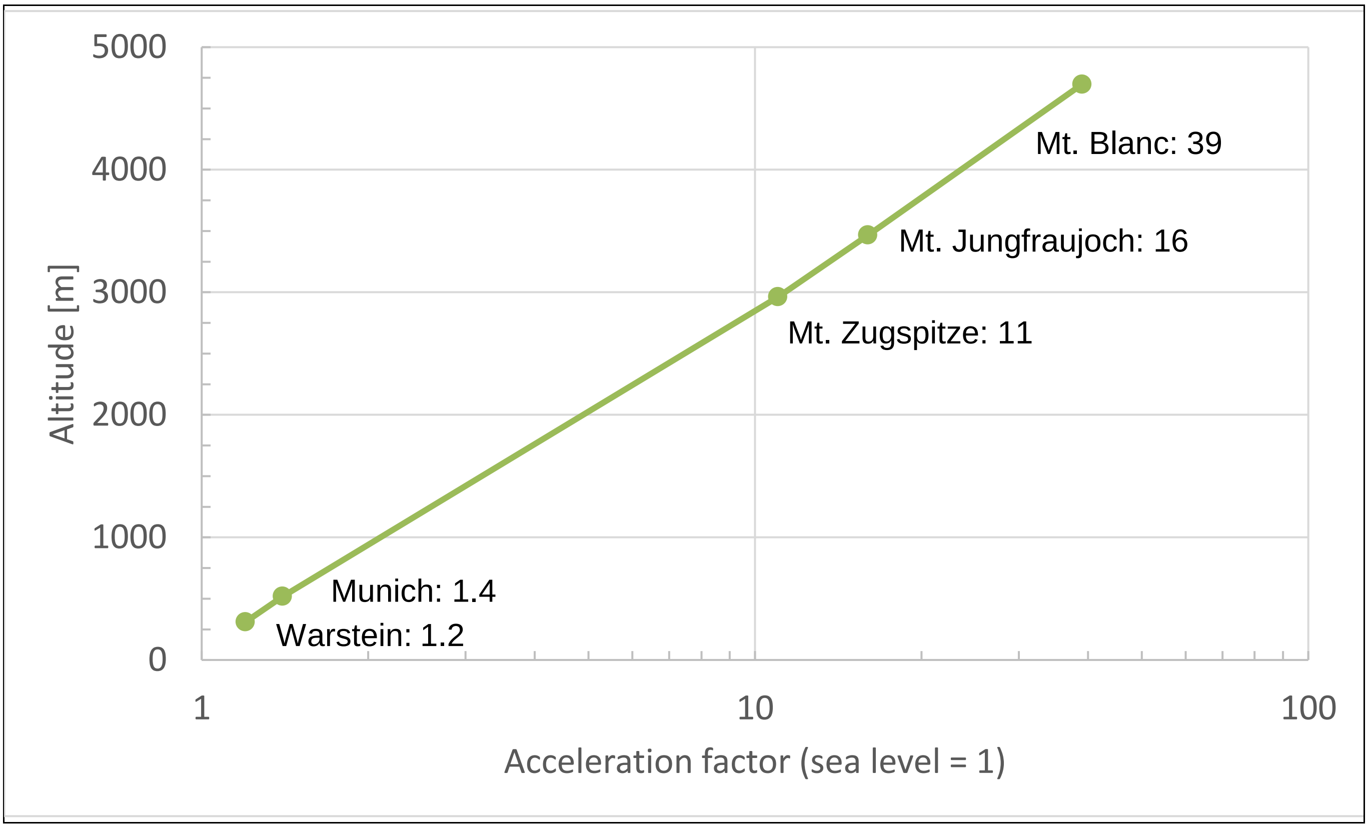

Figure 7 **Altitude dependency of acceleration factor with respect to known landmarks**

As already mentioned, in order to ensure a certain statistical confidence in the measurement result, it is necessary to wait for approximately 10 failures, while the probability of the occurrence of a failure exponentially depends on the drain-source blocking voltage. On the other hand, the typical application-relevant voltages are considerably lower than the $V_{(BR)DSS}$ (e.g., 520 V for $V_{(BR)DSS}$ = 650 V), meaning that waiting for eight or nine failures is not a viable option; for instance, 10 FIT/device means 1 fail out of 1000 devices in 10 years. In order to shorten the measurement time and have enough failures to get significant statistics at application-relevant voltages, testing with high-energy proton or neutron beams has been established as per the corresponding JEDEC specification JEP151 [4]. The available fluxes offer acceleration factors of up to 10^9. These enable the experimenter to conduct single runs in half an hour and sweep a certain range of parameters of bias voltage and junction temperature within one measurement campaign.

The measurement of cosmic radiation induced failure rates in accordance with JEP152 is part of Infineon's standard technology development process. Note that the artificial radiation sources used for accelerated measurements are able to reproduce only part of the natural spectrum (e.g., a limited energy spectrum or just one type of particle), and for this reason Infineon complements accelerated measurements with storage measurements to ensure the consistency of the data obtained with the two measurement methods.

3 Infineon generic mission profile for onboard chargers (OBCs)

An accurate mission profile is crucial to assess the robustness of the HV semiconductors within the harsh environment of automotive applications. This document presents a generic mission profile for an OBC/DC-DC converter based on certain practical assumptions.

The given mission profile assumes a bidirectional power flow for the applications.

More information about the process of robustness validation based on mission profiles can be found in literature, e.g., [5].

3.1 Operating modes

When the car is in driving mode, most of the onboard power electronics is in active operation. This is applicable to the HV-LV DC-DC converter, which connects the HV domain from the traction battery to the LV board net system. Nevertheless, the situation for the OBC is quite different. The traditional OBC is only active when the car is parked, an AC source is available and the battery management system demands energy to charge. Nonetheless, the picture changes when application scenarios like vehicle-to-load or even vehicle-to-grid are considered. Then, the OBC is not only responsible for charging the battery – but also providing the energy from the battery in the right format for the "outside world".

Table 1 shows the three most important operating modes for electric vehicles and defines the state of operation for the HV-LV DC-DC converter and the OBC.

Table 1 Operating modes

Mode	Comment	Technical implication
Parking	Electric vehicle is parked either with or without the charging cable attached to the AC grid	The OBC is off and separated from the AC input through electromechanical relay in the car. The HV-LV DC-DC converter is off and separated from the HV battery with the main relay.
Charging and cabin pre-conditioning	The HV battery is charged or discharged	The OBC is either working as a charger or as an inverter to provide AC on the charging interface. The HV-LV DC-DC converter is fully operational.
Driving	The car is in driving mode	The OBC is off and separated from the HV grid. The HV-LV DC-DC converter is fully operational.

3.2 Operating times

Based on Infineon's experience, a model of the operating times has been created to assess the failure rate of the power semiconductors in the OBC and HV-LV DC-DC subsystems. This is shown in **Table 2**.

Table 2 Assumed operating time per system

Mode	OBC status	HV LV DC-DC status	Operating time
Charging and cabin pre-conditioning: *The EV is connected to an AC outlet and the cabin is being pre-conditioned*	On	On	55000 hours
Driving *The EV is driving*	Off	On	8000 hours
Parking *The EV is parked but not charging (e.g., not connected via cable) and completely turned off*	Off	Off	68400 hours

Table 2 shows the operating time for the OBC. The assumption is that the bidirectional power flow capability leads to an increased number of charge and discharge cycles and, as a consequence, the hours of operation for the "charging and cabin pre-conditioning" profile have been significantly increased compared to unidirectional OBCs.

3.3 Temperature model

Another significant input for the calculation of the failure rate is the junction temperature of the HV power semiconductors. **Table 3** suggests such a temperature model for the above-mentioned operating modes. Please note that the FIT rate of the semiconductors is actually influenced by the junction temperature of the chip, which is coupled to the liquid cooling system of electric cars.

Table 3

Mode	Ambient temperature in °C	Relative time of operation
Charging and cabin pre-conditioning	-40	6%
	23	20%
	50	65%
	100	8%
	105	1%
Driving	30	1%
	40	10%
	50	18%
	60	27%
	70	35%
	80	8%
	90	1%
Parking e-car is off and not connected via cable	Junction temperature (T_j) is coupled to ambient temperature	0%

3.4 Altitude model

As mentioned earlier, a significant accelerator for cosmic radiation induced failures is the altitude where the HV power system is being operated.

For this reason, Infineon developed a model assuming the usage of electric cars based on the global distribution of the population over elevation. This model is presented in **Table 4**.

Table 4 **Altitude profile**

Operating time (relative)	Altitude in MSL
60%	600
25%	1500
10%	2000
5%	3250

3.5 Model of the HV subsystem

For accurate FIT results, it is relevant to describe the electrical conditions as precisely as possible, as well as the environmental conditions.

Figure 8 gives an overview of the HV subsystem’s OBC and HV-LV DC-DC converter. These subsystems should deliver the required amount of power to charge the HV and LV batteries.

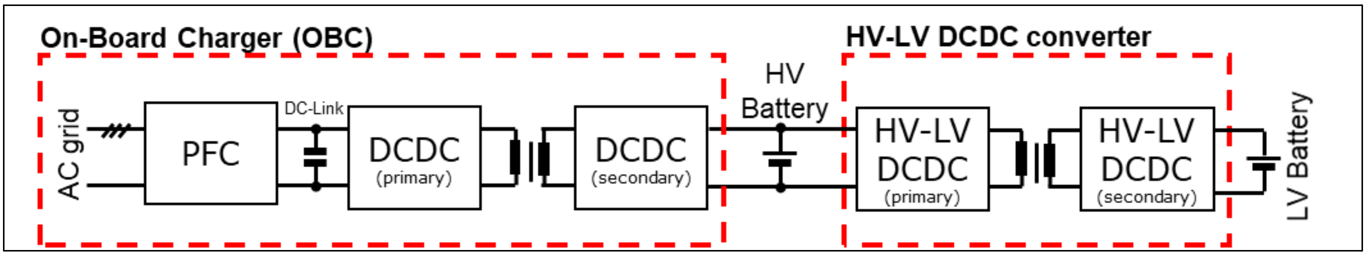

Figure 8 **Subsystems responsible for managing the power flow in a battery electric vehicle**

The OBC block (**Figure 8**, left side) provides energy to the HV battery by converting the AC at input voltage to the regulated DC voltage according to the battery charging profile. The AC input could be realized as single- or three-phase. For our purposes, we assume a single-phase input ($V_{in,max}$ = 265 V_{rms}).

Because we also consider vehicle-to-load scenarios, the OBC is assumed to be bidirectional. OBC can reverse its power flow direction: the AC grid becomes the load, while the HV battery acts like the energy source in this operating mode.

The right block in **Figure 8** shows the HV-LV DC-DC converter. As the name of this block indicates, it is converting a HV DC voltage to a LV DC voltage, and vice-versa. For the cosmic ray evaluation, we only consider the HV side of the DC-DC, as the cosmic radiation affects HV devices more severely. **Figure 9** indicates the blocks being considered for cosmic radiation assessment in red (these are the blocks that have HV power semiconductors).

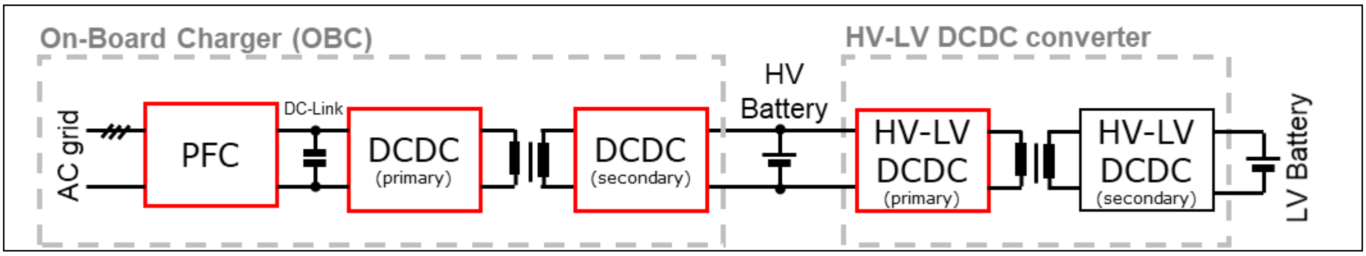

Figure 9 **Blocks highlighted in red are utilizing HV components and thus are considered in the cosmic radiation assessment**

As mentioned in the previous chapters, the hypothetical FIT of the HV power semiconductors within these power electronic systems is being evaluated for a use-case mission profile. If these blocks are in active operation, the semiconductors must be able to block the high voltages depending on the respective duty cycle output of the controller – this must be safeguarded under the environmental conditions and over the intended lifetime.

Two relevant voltage stress domains that can be identified by looking at the system in detail:

1. DC-link domain
2. HV-battery domain

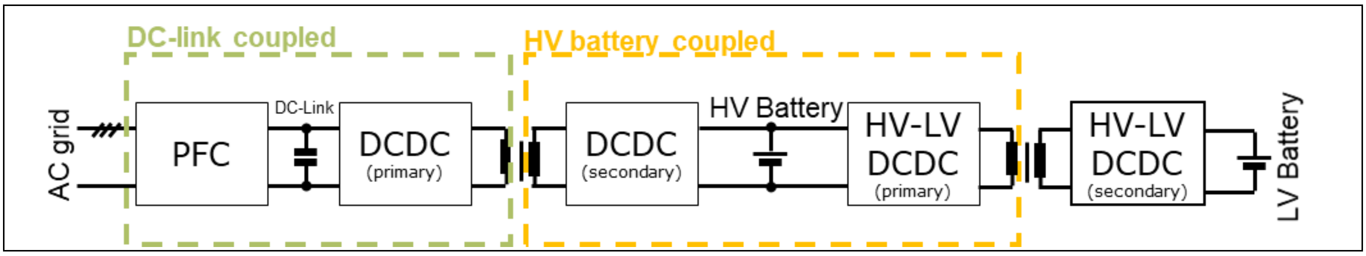

Figure 10 **Overview of the voltage stress domains**

Figure 10 highlights this dependence of the relevant stress voltage between the above-mentioned voltage domains. The next two chapters describe these sections in detail.

3.5.1 DC-link coupled voltage stress

The PFC and the primary side of the DC-DC stage of the OBC belong to the DC-link coupled domain. The relevant stress voltage is nominated as $V_{stress1}$, as **Figure 11** shows.

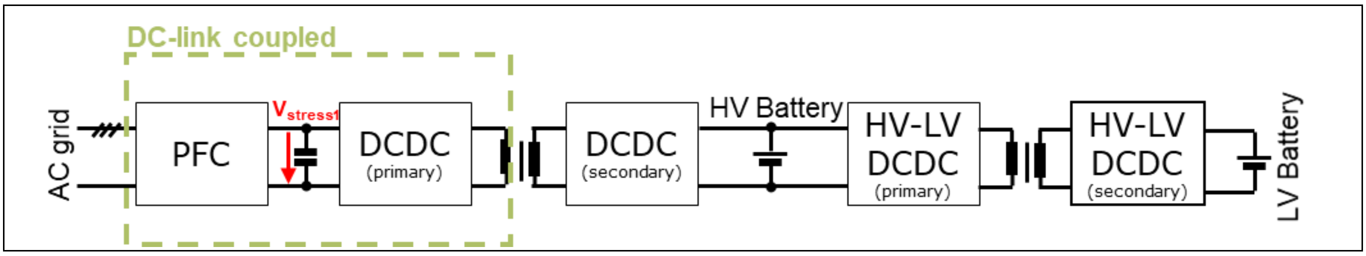

Figure 11 **$V_{stress1}$ is the variable modeling the behavior of the high voltage for the DC-link coupled blocks**

It is imperative to model the long-term conditions of the V_{stress} voltage as accurately as possible. Therefore, V_{stress} is set to the nominal DC-link voltage:

$$V_{stress1,nom} = 400\ V$$

Additionally, overshoot and abnormal conditions are assumed to be 80 percent of the rated breakdown voltage of the power MOSFET:

$$V_{stress1,os} = 520\ V$$

It is assumed that a rectangular overshoot voltage of 50 ns duration occurs at each switching cycle over the complete operating time of the OBC. The actual overshoot voltage depends on different parameters, such as PCB layout, package concepts, load point, and gate drive settings. Nevertheless, the simple rectangular model of the overshoot voltage is sufficient to assess the cosmic radiation robustness.

Additionally, a worst-case load-dump scenario is also included in the calculation. Also here, a simple rectangular voltage shape is assumed based on the field experience:

$$V_{stress1,ld} = 550\ V$$

Our model hypothesizes that these load dumps occur three times per lifetime and for 10 s duration each time.

3.5.2 HV battery coupled voltage stress

The secondary side of the DC-DC in the OBC and the primary side of the HV-LV DC-DC converter belong to the HV battery domain. The voltage to be considered for the cosmic radiation assessment is called $V_{stress2}$.

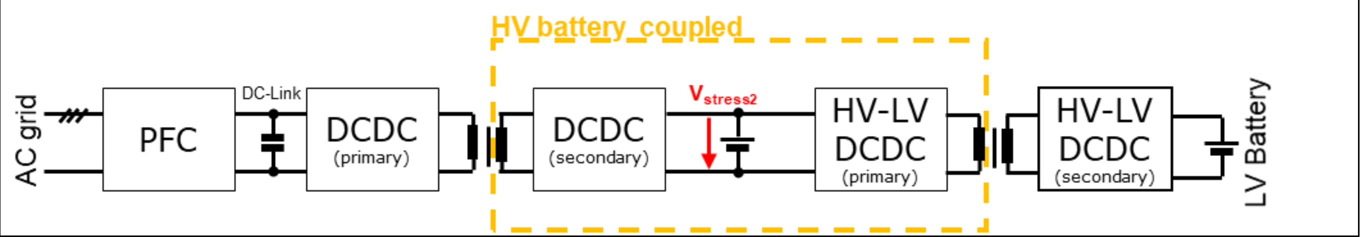

Figure 12 $V_{stress2}$ **is the variable modeling the behavior of the high voltage for the HV battery coupled blocks**

Similar to the previous section, a model of the stress voltage, $V_{stress2}$, is created. The difference is that this stress voltage depends mainly on the state of charge of the HV battery. **Figure 12** depicts the stress voltage and the dependent blocks. Here also a simple but conservative model is applied to reflect the voltage over lifetime.

We assume that for the majority of the time (90 percent), the battery operates at its full voltage:

$$V_{stress2} = 475\ V$$

For 9 percent of the time, we assume a voltage reflecting a lower state of charge:

$$V_{lowsoc} = 440\ V$$

And for the remaining 1 percent of the time a discharged battery is assumed:

$$V_{dischg} = 250\ V$$

Figure 13 summarizes these assumptions.

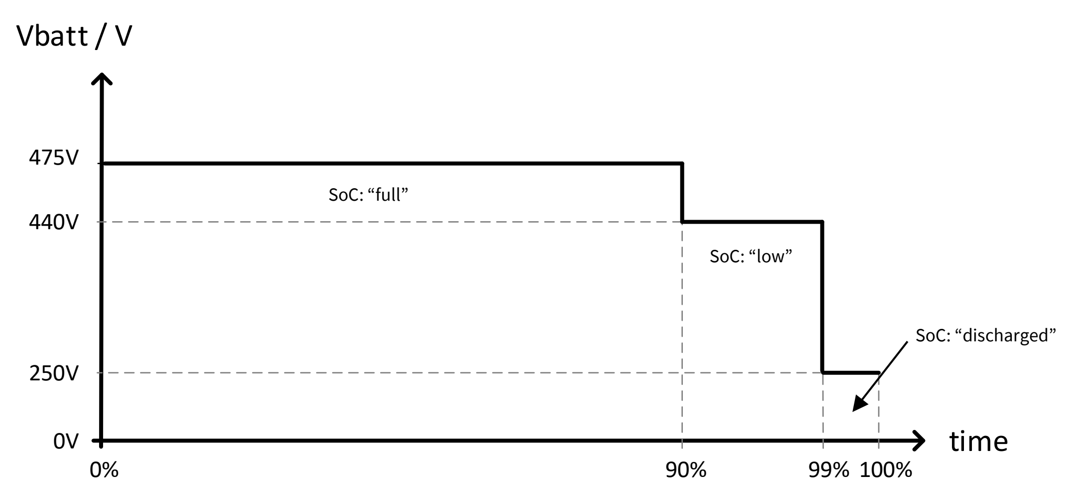

Figure 13 **Simple voltage model of the HV traction battery (time axis not included on scale for readability)**

Additionally, the transient voltages for the overshoot and the abnormal conditions as described in the previous chapter are considered.

3.5.3 Application conditions for different stages in the OBC

After having defined the electrical stress conditions for the OBC, the application parameters such as duty cycle and switching frequency also need to be defined, and are explained in **Table 5**.

The PFC block operates in continuous conduction mode (CCM). The assumed switching frequency for the PFC block is 100 kHz. The duty cycle varies between 3 percent and 97 percent over the AC input semi-cycles.

For the DC-DC stage in the OBC, we assume a full-bridge topology switching at maximal 500 kHz with a duty cycle of 50 percent.

For the HV-LV DC-DC block we assume a full-bridge topology with a maximum switching frequency of 500 kHz with a duty cycle of 50 percent – identical to the DC-DC stage in the OBC.

Table 5 **Worst-case assumptions for the HV subsystems**

Subsystem	Switching frequency (max.)	Duty cycle	Comment
PFC stage in OBC	100 kHz	3% … 97%	Totem pole PFC in CCM operation
DC-DC in OBC (HV-HV)	500 kHz	50%	Full-bridge resonant converter
HV-LV DC-DC	500 kHz	50%	Full-bridge resonant converter

4 Example results of cosmic radiation assessment

This chapter shows the results of the cosmic radiation assessment based on the previously described mission profile.

Two best-in-class products from Infineon's CoolMOS™ product family were selected as representative 650 V superjunction MOSFETs: **IPW65R048CFDA** (previous-generation CoolMOS™ automotive with fast body diode [6]) and **IPW65R022CFD7A** (CoolMOS™ automotive with fast body diode latest generation [7]). These products are perfectly suited to PFC and DC-DC stages within electric cars.

Table 6 shows the calculated FIT rate results for one CoolMOS™ device in the different sub-blocks of the HV subsystem.

Table 6 Expected typical FIT (number of fails per billion hours of operation) per CoolMOS™ semiconductor device rounded to 1 digit

Sub-block	Stress voltage domain	IPW65R022CFD7A FIT	IPW65R048CFDA FIT
PFC in OBC	DC-link	0	3
Primary side of DC-DC in OBC	DC-link	0	3
Secondary side of DC-DC in OBC	HV battery	0	70
Primary side of HV-LV DC-DC	HV battery	0	70
Secondary side of HV-LV DC-DC	LV battery	*Not relevant to consider*	*Not relevant to consider*

Table 6 shows that the **650 V CoolMOS™ CFD7A** technology is superior compared to the older generation **650 V CoolMOS™ CFDA** technology in terms of robustness against cosmic radiation. This unique feature of CoolMOS™ CFD7A becomes especially important if the board net voltages in the electric cars are up to 475 V battery voltage. CoolMOS™ CFDA is suitable for HV battery voltages up to about 420 V.

4.1 From devices FIT to application FIT

In reality, the complete AC-DC power conversion system consists of multiple power devices. To achieve a representative FIT rate on the system level, the results for the individual devices can be simply multiplied by the number of power semiconductors in their specific sub-block.

Figure 14 shows the power components of a typical OBC using CoolMOS™ CFD7A.

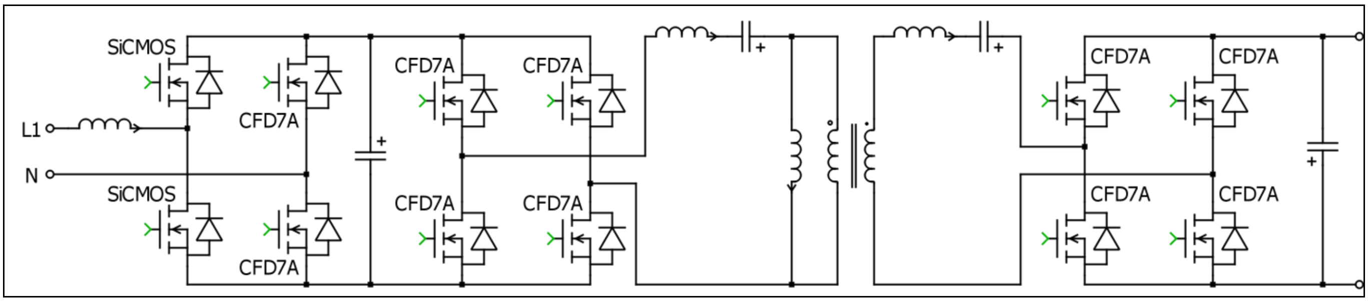

Figure 14 Single-phase bidirectional OBC comprising PFC and HV-HV DC-DC stage

Now, to calculate the correct total FIT rate, the two different stress voltage domains and the results from **Table 6** need to be considered. **Figure 15** shows the model of the voltage stress domains applied to the schematic level.

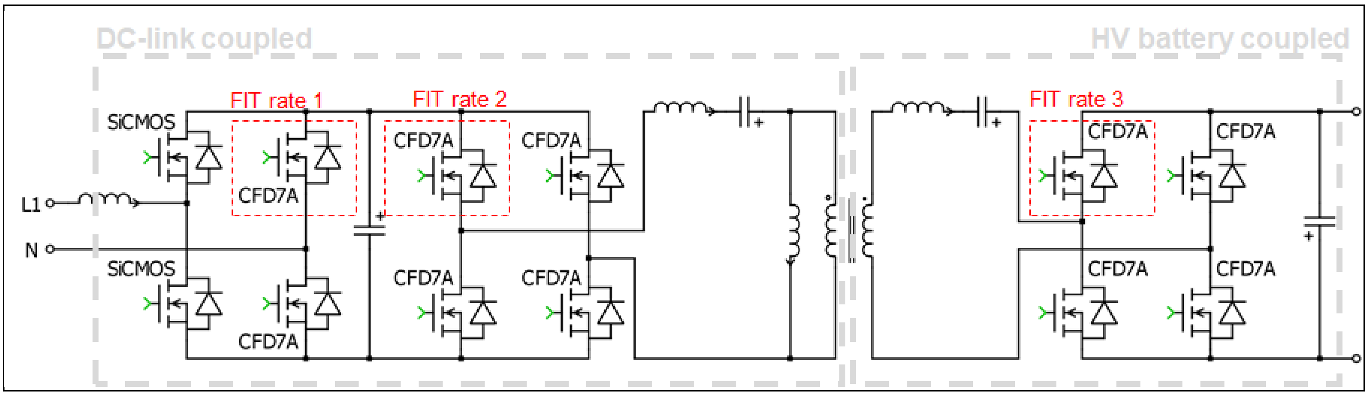

Figure 15 The relevant stress domains and the single device FIT in the single-phase bidirectional OBC

Based on **Figure 15**, the total FIT rate for each stress domain in the application can be calculated by multiplying the single device FIT rate with the respective number of devices. Subsequently, a sum of the intermediate results is created. **Table 7** summarizes these results.

As the results show, the total FIT rate for all CoolMOS™ CFD7A devices in this example is below the single digit range and is therefore negligible for further reliability analyses.

Table 7 Summary of results of FIT rates on individual block level and application level

Total FIT rate for CFD7A in this application	Sub-block	Number of CFD7A devices in sub-block	FIT rates
	PFC	2	0
	DC-DC primary	4	0
	DC-DC secondary	4	0
Sum of individual FIT rates			**0**

5 Conclusion

This application note explained the effect of cosmic radiation on HV power semiconductors and proposes a mission profile model for a bidirectional OBC. It becomes clear that cosmic radiation effects are important to consider in reliability assessments for HV power electronic systems.

A concrete example was shown, of how the individual FIT rate for devices within the OBC can be calculated, and how a total FIT rate for the application can be derived. Looking at the results of this evaluation, the superiority of the latest 650 V CoolMOS™ CFD7A becomes visible. In **Figure 6**, the FIT curves of two MOSFETs with similar $R_{DS(on)}$ belonging to the CFDA and CFD7A technology are compared. The superiority of the CoolMOS™ CFD7A series can be exploited in two ways:

1. Under the same blocking voltage conditions, CoolMOS™ CFD7A allows for a reduced FIT with respect to CoolMOS™ CFDA.
2. When defining a maximum target FIT as the criteria for the MOSFET technology selection, CoolMOS™ CFD7A allows for higher application voltages compared to CoolMOS™ CFDA.

As a consequence, higher system voltages at higher altitudes can be supported without compromising reliability.

Infineon offers to evaluate the robustness of our semiconductors in your specific application! Please get in contact with your Infineon sales team for specific information.

6 References

[1] G. Soelkner, “Ensuring the reliability of power electronic devices with regard to terrestrial cosmic radiation”, Microelectronics reliability (2015)

[2] J.F. Ziegler, “Terrestrial cosmic rays”, IBM Journal of Research and Development 40, 19–39 (1996)

[3] W. Kaindl, “Modellierung höhenstrahlungsinduzierter Ausfälle in Halbleiterleistungsbauelementen”, Dissertation TU München, S. 24ff. (2005)

[4] JEDEC test specification JEP151, “Test Procedure for the Measurement of Terrestrial Cosmic Ray Induced Destructive Effects in Power Semiconductor Devices”

[5] Zentralverband Elektrotechnik und Elektronikindustrie e.V., “Handbook for Robustness Validation of Semiconductor Devices in Automotive Applications”: https://www.zvei.org/fileadmin/user_upload/Presse_und_Medien/Publikationen/2015/mai/Handbook_for_Robustness_Validation_of_Semiconductor_Devices_in_Automotive_Applications__3rd_edition_/Robustness-Validation-Semiconductor-2015.pdf

[6] IPW65R048CFD7A – Infineon’s CoolMOS™ CFDA series: https://www.infineon.com/dgdl/Infineon-IPW65R048CFDA-DS-v02_00-en.pdf?fileId=db3a304336797ff90136ba294542255a

[7] Infineon’s CoolMOS™ CFD7A series – high-voltage superjunction MOSFET for automotive applications: https://www.infineon.com/cfd7a

Revision history

Document version	Date of release	Description of changes
V 1.0	15-06-2021	First release

Trademarks
All referenced product or service names and trademarks are the property of their respective owners.

Edition 2021-06-15

Published by

Infineon Technologies AG

81726 Munich, Germany

© 2021 Infineon Technologies AG.
All Rights Reserved.

Do you have a question about this document?

Email: erratum@infineon.com

Document reference
AN_2105_PL52_2106_154710

IMPORTANT NOTICE
The information contained in this application note is given as a hint for the implementation of the product only and shall in no event be regarded as a description or warranty of a certain functionality, condition or quality of the product. Before implementation of the product, the recipient of this application note must verify any function and other technical information given herein in the real application. Infineon Technologies hereby disclaims any and all warranties and liabilities of any kind (including without limitation warranties of non-infringement of intellectual property rights of any third party) with respect to any and all information given in this application note.

The data contained in this document is exclusively intended for technically trained staff. It is the responsibility of customer's technical departments to evaluate the suitability of the product for the intended application and the completeness of the product information given in this document with respect to such application.

For further information on the product, technology delivery terms and conditions and prices please contact your nearest Infineon Technologies office (**www.infineon.com**).

WARNINGS
Due to technical requirements products may contain dangerous substances. For information on the types in question please contact your nearest Infineon Technologies office.

Except as otherwise explicitly approved by Infineon Technologies in a written document signed by authorized representatives of Infineon Technologies, Infineon Technologies' products may not be used in any applications where a failure of the product or any consequences of the use thereof can reasonably be expected to result in personal injury.